

Nonlinear polarization conversion using microring resonators

Chris Fietz^{1,*} and Gennady Shvets¹

¹Department of Physics, The University of Texas at Austin, Austin, Texas 78712, USA

*Corresponding author: flounder@physics.utexas.edu

Received January 23, 2007; revised April 4, 2007; accepted April 9, 2007;
posted April 11, 2007 (Doc. ID 79239); published June 5, 2007

We present a design of a polarization converter between linear, circular, and elliptic accomplished with an on-chip high- Q dielectric microring resonator. Nonlinear polarization switching can be accomplished at modest input intensities because of the high-intensity compression in the ring. We predict an optical bistability effect making the polarization of the transmitted light dependent on its spectral or intensity history. © 2007 Optical Society of America

OCIS codes: 260.5430, 230.4320, 130.4310.

In the past few decades, a variety of tools have been developed as part of an effort to create an all-optical signal processing capability. Many of these components are made from microresonators including add-drop filters [1–3], all-pass filters [4], Boolean gates [5,6], and more. The integration of these and other all-optical components with one another, as well as with nonoptical devices, either requires or can benefit from control over the polarization of light signals.

Several methods are available for manipulating the orientation of linearly polarized light. Some methods introduce asymmetric defects into waveguides to rotate linear polarization [7,8]. Also, semiconductor optical amplifiers have been used for polarization rotation [9,10]. There are also ways of converting between linear and circularly polarized light. Using electro-optical effects, a converter has been demonstrated that can adjust the phase between perpendicular polarizations of light and give some control over polarization rotations.

We will demonstrate that a microring resonator can be designed to introduce a phase difference between two orthogonally polarized light signals, giving us the ability to convert between linear, circular, and elliptical polarizations. By making the convertor from a microring we gain all the usual advantages these structures provide, including economy of size, the ability to use current fabrication techniques, and frequency dependence due to resonance. By using simple geometries, the analysis of such microrings is quite simple, and their behavior should be very predictable. Finally, we show that, owing to the nonlinear Kerr effect in Si, the polarization of the transmitted signal exhibits a bistable behavior [11,12]. This effect allows us to use the microring as a switch that can exist in two different states determined by, for example, the header of a packet. Each of these states corresponds to a different polarization of transmitted signal.

For a dielectric waveguide horizontally coupled to a microring, the two polarizations that are parallel and perpendicular to the direction of coupling (TE, horizontal electric, and TM, vertical electric, respectively) couple independently to the ring according to the

standard microring equations: $\vec{E}_3 = r\vec{E}_2 + it\vec{E}_1$, $\vec{E}_4 = r\vec{E}_1 + it\vec{E}_2$, and $\vec{E}_2 = ae^{i\phi}\vec{E}_3$ [3,13]. Here r and t are coupling coefficients that are determined by the geometry of the waveguide and microring, their separation, and, as we will see, the polarization of the signal. The factors a and ϕ represent the field attenuation and the phase advance from a single turn around the ring. Energy compression in the ring is given by

$$\frac{|\vec{E}_3|^2}{|\vec{E}_1|^2} = \frac{t^2}{(1-ar)^2 + 4ar \sin^2(\phi/2)}, \quad (1)$$

and the phase advance by the signal after passing by the microring (assuming low ring losses by letting $a=1$) is given by

$$\Phi = \pi + \phi + 2 \tan^{-1} \left(\frac{r \sin \phi}{1 - r \cos \phi} \right). \quad (2)$$

The coupling constants r and t can be calculated by considering the following model. When a propagating mode in a single waveguide (for example, a vertically polarized mode) passes close to a microring, then it is no longer an eigenmode of this coupled waveguide system. It can instead be thought of as a superposition of bonding and antibonding modes of the coupled waveguide system [14]:

$$\begin{array}{|c|} \hline \uparrow \\ \hline \square \\ \hline \end{array} \begin{array}{|c|} \hline \square \\ \hline \end{array} = \frac{\begin{array}{|c|} \hline \uparrow \\ \hline \square \\ \hline \end{array} \begin{array}{|c|} \hline \uparrow \\ \hline \square \\ \hline \end{array} + \begin{array}{|c|} \hline \uparrow \\ \hline \square \\ \hline \end{array} \begin{array}{|c|} \hline \downarrow \\ \hline \square \\ \hline \end{array}}{\sqrt{2}}.$$

In the same way, a signal in the microring can be thought of as superposition:

$$\begin{array}{|c|} \hline \square \\ \hline \end{array} \begin{array}{|c|} \hline \uparrow \\ \hline \end{array} = \frac{\begin{array}{|c|} \hline \uparrow \\ \hline \square \\ \hline \end{array} \begin{array}{|c|} \hline \uparrow \\ \hline \square \\ \hline \end{array} - \begin{array}{|c|} \hline \uparrow \\ \hline \square \\ \hline \end{array} \begin{array}{|c|} \hline \downarrow \\ \hline \square \\ \hline \end{array}}{\sqrt{2}}.$$

It was confirmed numerically that these simple expansions are accurate approximations of the actual single waveguide modes.

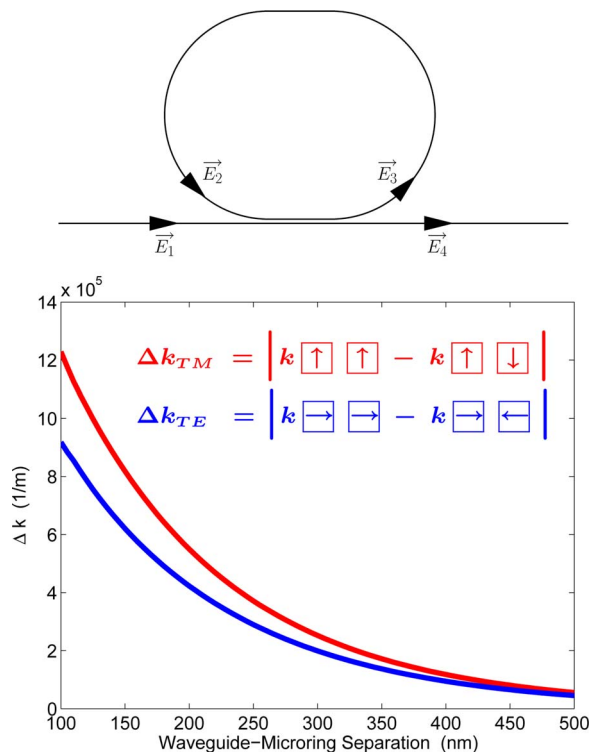


Fig. 1. (Color online) Dependence of Δk_{TM} and Δk_{TE} on the separation distance between the waveguide and microring. Both the waveguide and the ring are made of Si, have $300 \text{ nm} \times 300 \text{ nm}$ cross sections and are embedded in SiO_2 .

If these bonding and antibonding modes have different propagation constants, then after this superposition is allowed to propagate some effective distance D_{eff} the signal will begin to mix between being completely in the waveguide and completely in the microring. The mixing occurs with the beat $\Delta k = |k_{bond} - k_{anti}|$, the difference between the propagation of the bonding and antibonding modes. The coupling coefficients can then be expressed as

$$r = \cos\left(\frac{\Delta k D_{eff}}{2}\right), \quad t = \sin\left(\frac{\Delta k D_{eff}}{2}\right), \quad (3)$$

where D_{eff} is controlled by adjusting the microring radius or by elongating the ring into a racetrack. This model clarifies why only the waveguide modes whose polarizations are parallel and perpendicular to the coupling direction interact independently with the microring. For the vertically coupled [15] ring and waveguide, the same two polarizations of the waveguide, TE and TM, would independently interact with the ring. However, for the *diagonally* coupled ring and waveguide, we would have diagonal polarizations independently coupling to the ring. Thus, the TE- and TM-polarized modes of the waveguide would couple through their interaction with the ring, causing the outgoing light to be a superposition of the two modes, i.e., changing its polarization. Likewise, the waveguide mode initially polarized at 45° to the horizontal plane will change its polarization after interacting with a laterally coupled ring. This will be the configuration considered in this Letter.

The idea of using a microring to convert the polarization of light relies on designing a waveguide-microring pair whose coupling is polarization dependent. Here we consider a Si waveguide that has a square cross section and is embedded in SiO_2 , making the two polarizations degenerate and allowing us to send a signal polarized at an angle of 45° past the microring. For simplicity, the microring's cross section is also assumed to be square. If TE and TM polarizations have different coupling coefficients, then, according to Eq. (2), each polarization acquires a different phase shift after the microring. The phase difference between the two polarizations is

$$\Delta\Phi = 2 \tan^{-1} \left[\frac{r_{TM} \sin \phi}{1 - r_{TM} \cos \phi} \right] - 2 \tan^{-1} \left[\frac{r_{TE} \sin \phi}{1 - r_{TE} \cos \phi} \right]. \quad (4)$$

This equation assumes that $\phi_{TM} = \phi_{TE}$. The curvature of the microring actually splits the degeneracy of the two polarizations, but numerical estimates indicate that this splitting is small ($\Delta k/k < 10^{-6}$). This also means that the polarizations will not mix while traveling around the microring. Figure 1 shows that the dependence of Δk on waveguide-microring separation is approximately exponential. Although this figure is for a particular waveguide-microring geometry, its shape is typical for many different geometries. The difference between TE and TM mode coupling strengths to the ring is appreciable only for small waveguide-ring separations.

As an example, we designed a model microring to perform linear to circular polarization conversion ($\Delta\Phi = \pm \pi/2$). Assuming the 300 nm square waveguide and microring made of Si embedded in SiO_2 , we choose the ring radius and racetrack length to be 5 and $3 \mu\text{m}$ and set the separation distance between the waveguide and racetrack to be 400 nm . From Eq. (3) we obtain $r_{TE} = 0.9832$, $r_{TM} = 0.9140$, and, assuming losses of 10 dB/cm in Si, $\alpha = 0.9957$. Relative phase difference $\Delta\Phi$ and intensity compression in the ring (total and for each polarization) are plotted in Fig. 2. Figure 2 demonstrates that three conditions necessary for linear to efficient circular conversion are simultaneously satisfied for two specific wavelengths: (i) $\Delta\Phi = \pm \pi/2$, (ii) transmission losses are low, and (iii) matched for the two polarizations. Matching transmission losses is important for linear-to-circular and linear-to-linear polarization conversions.

High-energy compression (of order 30) at the polarization conversion frequencies indicated by Fig. 2 suggests that the nonlinear Kerr effect can be profitably exploited to accomplish nonlinear polarization control [11,12]. The nonlinear Kerr effect manifests itself as an increase in the phase advanced by the light traveling around the ring according to $\phi = C(k_0 + \gamma P_r)$, where, for simplicity, free-carrier and thermal effects have been neglected. Here C is the circumference of the ring, k_0 is the propagation constant ex-

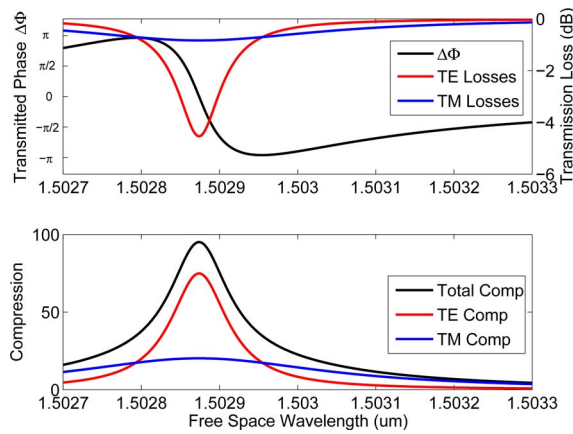


Fig. 2. (Color online) Top, $\Delta\Phi$ and transmission losses versus wavelength; bottom, energy compression versus wavelength. Peak losses are greater for the TE mode because it is closer to critical coupling ($r=a$) than the TM mode.

cluding nonlinear effects, P_r is the cross-sectional power in the ring directly proportional to the field intensity $|\vec{E}_3|^2$, and $\gamma=722.8/(W\text{ m})$. γ was found numerically by solving for the propagation constant k in the waveguide for varying intensities using $\chi_3=8.28 \times 10^{-19}\text{ m}^2/\text{V}^2$ [16]. As shown below, this nonlinear phase shift results in the optical bistability of the polarization of transmitted radiation.

Equation (1) was self-consistently solved with that for ϕ , and the resulting nonlinear phase shift $\Delta\Phi$ and transmission loss for each mode are plotted in Fig. 3 as a function of the wavelength for a fixed input power of $P_{in}=40\text{ mW}$ (top) and as a function of the input power for a fixed wavelength $\lambda=1.5031\text{ }\mu\text{m}$ (bottom). As before, the initial polarization at 45° was assumed. For a range of input power levels and wavelengths, these solutions are multivalued, indicating optical bistability. Specifically, we consider two cases: wavelength sweep and power sweep. For those wavelengths corresponding to multiple solutions, polarization of the transmitted signal depends on its

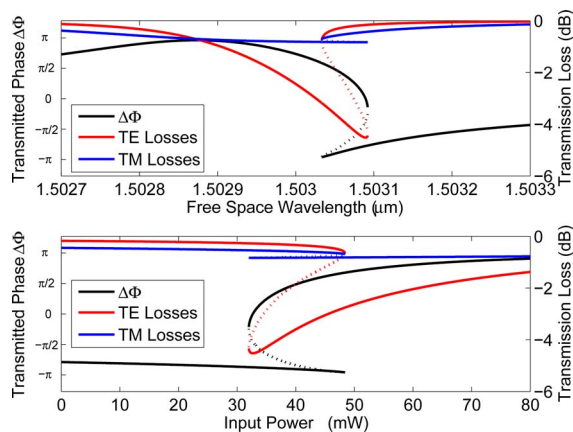


Fig. 3. (Color online) Top, $\Delta\Phi$ and transmission losses versus wavelength at $P=40\text{ mW}$. Bottom, $\Delta\Phi$ and transmission losses versus power at $\lambda=1.5031\text{ }\mu\text{m}$. Dashed curves correspond to physically unattainable (unstable) solutions.

history. If the input power is held constant while the wavelength is scanned upward, the TE component of the signal will be slightly damped in the multivalued region resulting the linear (TM) polarization of the transmitted signal. As the wavelength is scanned past the multivalued region, the losses will fall to the lower value. If the wavelength is scanned downward, losses will remain low, the relative phase shift will be $\Delta\Phi \approx -\pi/2$, and the transmitted polarization will be circular. Similar bistable effects can be accomplished by sweeping the input power as shown in Fig. 3(b). Note that the intermediate state of moderate losses represented in Fig. 3 by a dashed curve is unstable and physically unattainable. Given the bistable behavior of this converter, it is possible to use the converter as a switch. For example, two types of pulse header can be designed that bring the polarization of the transmitted signal into one of the two polarization states.

In summary, we have demonstrated that an on-chip dielectric microring resonator can be used to convert the polarization of light signals. By exploiting the nonlinear Kerr effect in Si, a polarization converter can be designed that exhibits optical bistability. This can be used to make a converter that has two different possible polarization outputs depending on the spectral or intensity history of the input.

This work was supported in part by the U.S. Army Research Office MURI grant W911NF-04-01-0203.

References

1. B. E. Little and S. T. Chu, *Opt. Photon. News* **11**(11), 24 (2000).
2. G. Griffel, *IEEE Photon. Technol. Lett.* **12**, 1642 (2000).
3. F. Xia, L. Sekaric, and Y. Vlasov, *Opt. Express* **14**, 3872 (2006).
4. C. K. Madsen and G. Lenz, *IEEE Photon. Technol. Lett.* **10**, 994 (1998).
5. T. A. Ibrahim, R. Grover, L.-C. Kuo, S. Kanakaraju, L. C. Calhoun, and P.-T. Ho, *IEEE Photon. Technol. Lett.* **15**, 1422 (2003).
6. T. A. Ibrahim, K. Amarnath, L. C. Kuo, R. Grover, V. Van, and P.-T. Ho, *Opt. Lett.* **29**, 2779 (2004).
7. Y. Shani, R. Alferness, T. Koch, U. Koren, M. Oron, B. I. Miller, and M. G. Young, *Appl. Phys. Lett.* **59**, 1278 (1991).
8. J. J. G. M. van der Tol, F. Hakimzadeh, J. W. Pedersen, D. Li, and H. van Brug, *IEEE Photon. Technol. Lett.* **7**, 32 (1995).
9. R. Manning, A. Antonopoulos, R. L. Roux, and A. Kelly, *Electron. Lett.* **37**, 229 (2001).
10. H. Soto, D. Erasme, and G. Guekos, *IEEE Photon. Technol. Lett.* **11**, 970 (1999).
11. O. Ogusu, *IEEE J. Quantum Electron.* **32**, 1537 (1996).
12. Q. Xu and M. Lipson, *Opt. Lett.* **31**, 341 (2006).
13. J. E. Heebner and R. W. Boyd, *Opt. Lett.* **24**, 847 (1999).
14. N. W. Ashcroft and N. D. Mermin, *Solid State Physics* (Thompson Learning, 1976).
15. S. J. Choi, K. Djordjev, S. J. Choi, P. D. Dapkus, W. Lin, G. Griffel, R. Menna, and J. Connolly, *IEEE Photon. Technol. Lett.* **16**, 828 (2004).
16. D. R. Lide, ed., *CRC Handbook of Chemistry and Physics* 87th ed. (CRC, 2006).